Development/Plasticity/Repair

Drosophila cacophony Channels: A Major Mediator of Neuronal Ca^{2+} Currents and a Trigger for K^+ Channel Homeostatic Regulation

I-Feng Peng and Chun-Fang Wu
Department of Biological Sciences, University of Iowa, Iowa City, Iowa 52242

The *cacophony* (*cac*) locus in *Drosophila* encodes a Ca^{2+} channel α subunit, but little is known about properties of *cac*-mediated currents and functional consequences of *cac* mutations in central neurons. We found that, in *Drosophila* cultured neurons, Ca^{2+} currents were mediated predominantly by the *cac* channels. The *cac* channels contribute to low- and high-threshold, fast- and slow-inactivating types of Ca^{2+} currents, take part in membrane depolarization, and strongly activate Ca^{2+}-activated K^+ current [$I_{K(Ca)}$]. In *cac* neurons, unexpectedly, voltage-activated transient K^+ current I_A is upregulated to a level that matches $I_{K(Ca)}$ reduction, implicating a homeostatic regulation that was mimicked by chronic pharmacological blockade of Ca^{2+} currents in wild-type neurons. Among K^+ channel transcripts, *Shaker* mRNA levels were preferentially increased in *cac* flies. However, Ca^{2+} current expression levels remained unaltered in several K^+ channel mutants, illustrating a key role of *cac* in developmental regulation of *Drosophila* neuronal excitability.

Key words: cac; Dmca1A; ion channel regulation; real-time PCR; compensatory regulation; Ca channel mutations

Introduction

Ca^{2+} influx through voltage-gated Ca^{2+} channels regulates neuronal membrane excitability, synaptic transmission, plasticity, and growth. A large family of these channels has been identified molecularly and classified according to their gating kinetics, single-channel conductances, and pharmacological profiles (Catterall, 2000; Ertel et al., 2000; Hille, 2001). Five high-threshold, slow-inactivating subtypes (L, N, P, Q, and R), together with the low-threshold, fast-inactivating T-type, form the major Ca^{2+} entry pathway in mammalian excitable cells. Clustered Ca^{2+} channel activities lead to intracellular high-Ca^{2+} microdomains (Llinas et al., 1981), contribute to membrane depolarization, and activate local Ca^{2+}-activated K^+ current [$I_{K(Ca)}$] (Gola and Crest, 1993; Robitaille et al., 1993; Marrion and Tavalin, 1998; Vergara et al., 1998). Voltage-dependent K^+ currents, including inactivating I_A and non-inactivating I_K (for review, see Coetzee et al., 1999), can also be modulated during increases in internal Ca^{2+}. For example, modifications of I_A or I_K channels, induced by behavior conditioning or excitability change, are triggered by cyclic nucleotide- and/or protein kinase-related mechanisms (Alkon et al., 1982; Poulain et al., 1994; Enyeart et al., 1996; Yao and Wu, 2001).

Homeostasis highlights the ability of biological systems to adjust the internal physiological milieu in response to external perturbations (Cannon, 1932). It has been documented in a number of preparations that, after experimental manipulations of membrane excitability or synaptic activity, some neurons are capable of maintaining appropriate levels of excitation over time by various compensatory mechanisms, including Ca^{2+}-dependent regulations of ion channel function and synaptic efficacy (Spitzer, 1999; Turrigiano, 1999; Davis and Bezprozvanny, 2001; Marder and Prinz, 2002). The complex long-term homeostatic effects caused by altering Ca^{2+} influx, as well as the genetic control of the diversity of Ca^{2+} channels, can be further investigated in established genetic systems.

In *Drosophila*, neuronal Ca^{2+} currents are also composed of low-threshold, fast-inactivating and high-threshold, slow-inactivating components (Byerly and Leung, 1988; Saito and Wu, 1991; Schmidt et al., 2000). Two genes, *Dmca1D* and *cacophony* (*cac*, or *Dmca1A*), are known to encode Ca^{2+} channel α subunits in *Drosophila* (Zheng et al., 1995; Smith et al., 1996). They play major but nonredundant roles because null alleles of each cause embryonic lethality (Smith et al., 1996; Eberl et al., 1998). *Dmca1D* encodes vertebrate L-type-like channels, which are enriched in muscles for mediating dihydropyridine (DHP)-sensitive Ca^{2+} current (Gielow et al., 1995; Zheng et al., 1995; Ren et al., 1998). The *cac* locus, identified in a mutant screen for altered courtship song (von Schilcher, 1976), encodes Ca^{2+} channels homologous to vertebrate N-, P-, and Q-type channels (Smith et al., 1996; Rieckhof et al., 2003). It is thought that *cac* is expressed in the nervous system, as indicated by the reduced synaptic efficacy and altered motor terminal growth at neuromuscular junctions in several viable *cac* alleles (Kawasaki et al., 2000, 2002, 2004; Rieckhof et al., 2003; Kuromi et al., 2004). However, how *cac* channels mediate the diverse neuronal Ca^{2+}

Received Oct. 31, 2006; revised Dec. 20, 2006; accepted Dec. 21, 2006.

This work was supported by National Institutes of Health Grants HD18577 and NS26528. We thank Dr. J. Miller and Dr. J. Lin for the advice and support on real time-PCR experiments. We also thank J. Lee for comments on this manuscript.

Correspondence should be addressed to Chun-Fang Wu, Department of Biological Sciences, University of Iowa, Iowa City, IA 52242. E-mail: chun-fang-wu@uiowa.edu.

DOI:10.1523/JNEUROSCI.4746-06.2007

 0270-6474/07/271072-11$15.00/0

currents and how *cac* mutations affect other ion currents have not been determined under voltage- and current-clamp conditions.

In this study, we isolated inward Ca^{2+} and outward K^+ currents by performing whole-cell clamp recordings on cultured "giant" neurons differentiated from cytokinesis-arrested embryonic neuroblasts of *Drosophila* (Wu et al., 1990; Zhao and Wu, 1997; Yao and Wu, 1999). Our results demonstrate that *cac* mutations greatly suppressed neuronal Ca^{2+} currents of different biophysical properties. Striking alterations were also observed in different types of K^+ currents: a great decrease in $I_{K(Ca)}$ coupled with an increase in I_A but with no changes in I_K. Additional pharmacological and molecular approaches were adopted to investigate a potential homeostatic mechanism of I_A upregulation in *cac* neurons.

Materials and Methods

Drosophila *stocks.* The wild-type (WT) strain was Canton S. A homozygous viable allele cac^s (Smith et al., 1996) (from Dr. J. Hell, Brandies University, Waltham, MA) and a *cac* deficiency line $l(1)L13^{HC129}/In(1)FM7i, P\{w^{+wC} = Act\ GFP\}$ (Kawasaki et al., 2002) (from Dr. R. Ordway, Pennsylvania State University, University Park, PA) were examined. The experiments also included Sh^M [*Shaker*^{M}, a null allele (Zhao et al., 1995)], $Shab^3$ [*Shaker cognate b*^{3}, a null allele (Singh and Singh, 1999)], and slo^1 [*slowpoke*^{1}, a hypomorph (Elkins et al., 1986)]. The slo^1 chromosome also carried a visible marker *scarlet*.

Single-embryo giant neuron culture. The giant neuron culture system has been described previously (Saito and Wu, 1991; Zhao and Wu, 1997; Yao and Wu, 1999, 2001; Berke and Wu, 2002). Briefly, the interior content of stage 7–8 embryos was sucked out with a glass micropipette and then dispersed in culture medium on an uncoated coverslip. The culture medium contains 80% *Drosophila* Schneider medium and 20% fetal bovine serum (both from Invitrogen, Carlsbad, CA), with the addition of 200 ng/ml insulin, 50 μg/ml streptomycin, and 50 U/ml penicillin (all from Sigma, St. Louis, MO). To generate giant neurons from neuroblasts, cytochalasin B (CCB) (2 μg/ml; Sigma) was added on the first day to arrest cytokinesis (Wu et al., 1990). Within 1 d after CCB washout, phalloidin staining shows restoration of actin filament structures coupled with profuse growth of filopodia and expanded lamellipodia (Berke et al., 2006). For chronic or acute pharmacological effects, cultures were raised in or treated with media containing the drugs at the final concentrations specified. These drugs included amiloride, NiCl, apamine (all from Sigma), and charybdotoxin (Alomone Labs, Jerusalem, Israel). Before electrophysiological recording, drugs were washed out by standard bath solution (see below).

Electrophysiology. Whole-cell patch-clamp recording from cultured giant neurons has been described previously (Saito and Wu, 1991; Zhao and Wu, 1997; Yao and Wu, 1999, 2001). Recording electrodes prepared from 75 μl glass micropipettes (VWR Scientific, Chicago, IL) had a tip opening of ~1 μm and an input resistance of 3–5 MΩ in bath solution. The normal pipette solution contained the following (in mM): 144 KCl, 1 $MgCl_2$, 0.5 $CaCl_2$, and 5 EGTA, buffered at pH 7.1 with 10 HEPES. For inward current measurement, K^+-free (replaced by Cs^+) pipette solution was used to reduce outward K^+ current contamination. The standard bath solution contained the following (in mM): 128 NaCl, 2 KCl, 4 $MgCl_2$, 1.8 $CaCl_2$, and 35.5 sucrose, buffered at pH 7.1 with 5 HEPES. To facilitate measurements of currents through Ca^{2+} channels, Ba^{2+} (from 5 to 20 mM, as indicated) was added to serve as a charge carrier, with additional blockers for Na^+ channels (10 nM TTX; Sankyo, Tokyo, Japan) and K^+ channels [1 mM 4-AP (Sigma), 0.05 mM quinidine (Sigma), and 2.5 mM tetraethylammonium (TEA) (Eastman Kodak, Rochester, NY)]. Recordings were performed on the soma of neurons (diameters ranging from 15 to 18 μm) in 2- to 3-d-old cultures by using a patch-clamp amplifier (Axopatch 1B; Molecular Devices, Palo Alto, CA). The seal resistance was usually >5 GΩ, and junction potentials were nulled before establishing the whole-cell configuration. A personal computer in conjunction with an analog-to-digital converter and pClamp software (version 5.5.1; Molecular Devices) was used to generate the current- and voltage-clamp commands and for data acquisition. All experiments were done at room temperature. Current densities were normalized to membrane capacitance, which was obtained by using a small hyperpolarization step (−4 mV, 25 ms). To determine steady-state inactivating current, the test pulse (+60 mV) was delivered 5 ms after 500 ms preconditioning pulses varying from −100 to +60 mV at 20 mV increments. The computer program for analyzing dV/dt of "Ca^{2+} spikes" (see Fig. 3*D*) was created with C++ Language (Borland, Scotts Valley, CA).

Quantification of mRNA levels of K^+ channel genes. Primers for real-time (RT)-PCR detection of the target genes were designed by using PrimerExpress software of Applied Biosystems (Foster City, CA) and were synthesized by Integrated DNA Technology (Coralville, IA). The primers specifically probe the conserved domains of individual genes reported in current updates in FlyBase (http://flybase.bio.indiana.edu/) and are expected to detect all splice variants for each gene. FlyBase identification numbers are as follows: *Sh*, FBgn0003380; *Shal* (*Shaker cognate l*), FBgn0005564; *slo*, FBgn0003429; and *SK* (small conductance calcium-activated potassium channel), FBgn0029761. The primer sequences were as follows (F, forward; R, reverse; 5′ to 3′): glyceraldehyde-3-phosphate dehydrogenase (GAPDH)-F, 5′-AGCGCTGGTGCCGAATAC-3′; GAPDH-R, 5′-AGTGAGTGGATGCCTTGTCGAT-3′; *Sh*-F, 5′-CGGATAATGAGAAACAGAGAAAAGTCT-3′; *Sh*-R, 5′-TGGCGGCTTGCGAACT-3′; *Shal*-F, 5′-CCAGAGACAATAGCTGGCAAAA-3′; *Shal*-R, 5′-GACCAGCACACCGCTAAGC-3′; *slo*-F, 5′-AAAGACTGGGCTGGAGAGCTT-3′; *slo*-R, 5′-AACGACCAAAATTCGACCAGTT-3′; *SK*-F, 5′-GCGAAAGGTTCCACGATGAG-3′; and *SK*-R, 5′-GCCGTTAGCCACATGGAGTT-3′.

Flies 1–2 d after eclosion of individual genotypes were frozen in liquid nitrogen, and their heads were detached by a 10 s vortexing. Fifty to 55 heads were grounded in a 2 ml homogenizer, and total RNA was extracted by using the RNeasy Mini kit (Qiagen, Valencia, CA). An on-column DNase digestion was performed during RNA preparation to remove potential genomic DNA contamination. Reverse transcription was performed using the SuperScript III kit (Invitrogen) with random primers. The copies of double-stranded (ds) DNAs containing the conserved domain corresponding to the individual K^+ channel probes were amplified in PCR in proportion to the initial abundance. Using Power SYBR Green PCR Master Mixer (Qiagen), the fluorescent reaction products were quantified optically with an ABI Prism 7000 machine (Applied Biosystems). For each reaction, a single PCR product was indicated by a characteristic dsDNA dissociation temperature. Triplicates of PCR runs were performed for each gene on each of the three independent RNA preparations. The abundance of transcripts for individual K channel genes was determined by normalizing their optical measurements to that of GAPDH from the same genotypes (Guan et al., 2005).

Results

Currents mediated by Ca^{2+} channels in cultured *Drosophila* giant neurons

Whole-cell voltage-clamp recordings were performed on *Drosophila* giant neuron cultures to investigate the currents flowing through Ca^{2+} channels. Ca^{2+} currents (I_{Ca}) were indicated by the remaining inward current measured in TTX-containing (10 nM) standard bath solution and K^+-free (replaced by Cs^+) pipette solution (Fig. 1*A*). During a depolarization step from −80 to 0 mV, a small inward current could be detected in WT neurons. An elevated external Ca^{2+} (from 1.8 to 5.0 mM) increased the amplitude of this inward current. The response turned outward beyond an extreme positive voltage of above +40 mV (Fig. 1*A*), presumably reflecting some remaining Ca^{2+}-activated K^+ currents [similar to the observations in other *Drosophila* preparations (Byerly and Leung, 1988)]. Ba^{2+} is known to be a more effective charge carrier through Ca^{2+} channels (Hille, 2001). Adding Ba^{2+} in the bath solution further enhanced the inward current on the same cell and suppressed the outward currents at +40 mV (Fig. 1*A*). In addition, adding Ba^{2+} also affected action potential shape and firing pattern (Fig. 1*B*). We regularly ob-

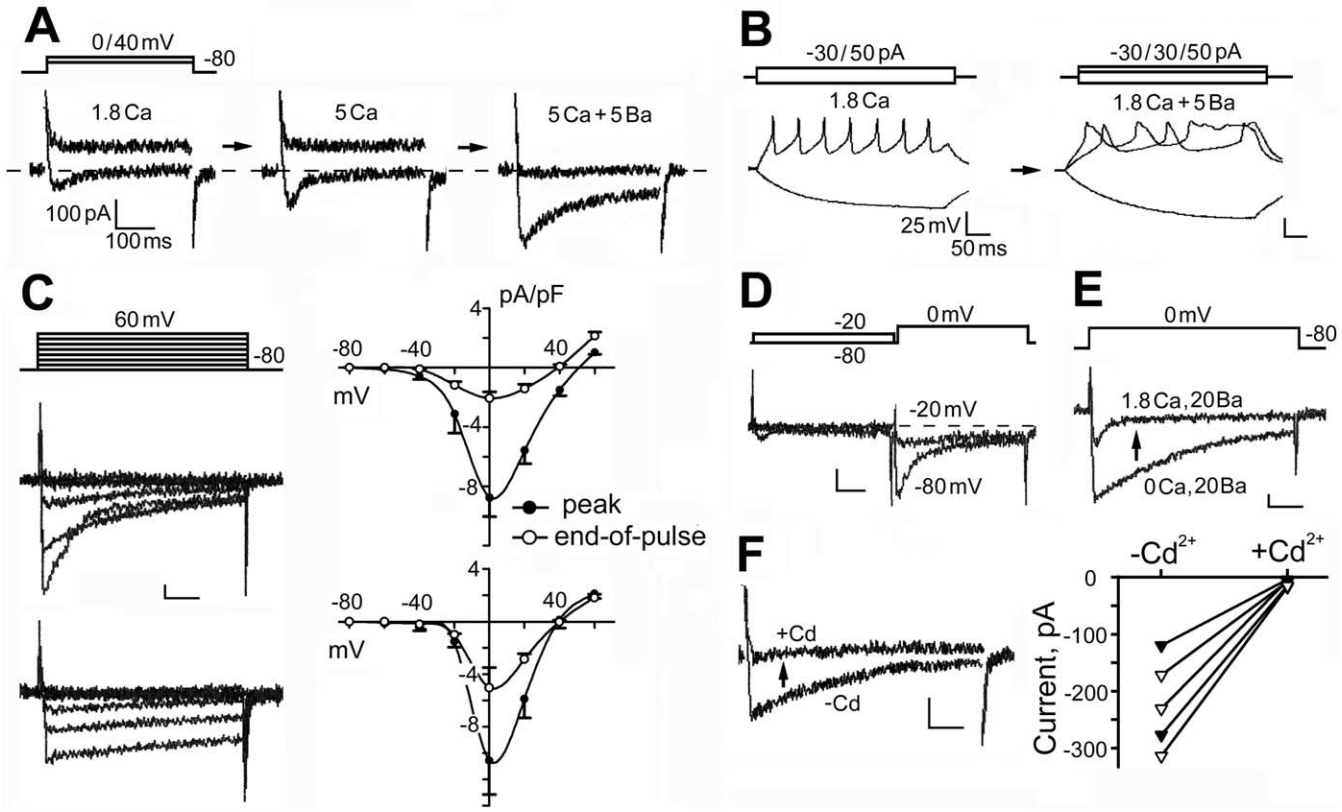

Figure 1. Properties of Ca^{2+} channels in cultured *Drosophila* giant neurons. ***A***, Whole-cell voltage clamping of Ca^{2+} currents in standard bath solution containing TTX to block Na^+ current, with K^+ currents suppressed by using K^+-free, Cs^+ pipette solution. Superimposed current traces elicited by voltage-clamp steps from −80 to 0 and +40 mV are shown. The amplitude of inward currents (I_{Ca}) at 0 mV increased with the elevation of extracellular Ca^{2+} (from 1.8 to 5 mM). An additional 5 mM Ba^{2+} further enhanced the inward current [$I_{Ba(Ca)}$]. Note the suppression of outward currents at +40 mV by Ba^{2+} application. ***B***, Spike trains initiated during current clamping in standard bath solution. Note broadening of the action potentials after 5 mM Ba^{2+} application. ***C***, Kinetics and voltage dependence of $I_{Ba(Ca)}$. To isolate inward currents, standard bath solution contained 20 mM Ba^{2+}, 1.8 mM Ca^{2+}, TTX, 4-AP, TEA, and quinidine (see Materials and Methods). As shown in the two sets of superimposed current traces, two distinct kinetic components of $I_{Ba(Ca)}$ were evident, which displayed fast versus slow inactivation (τ of $<$100 vs $>$300 ms at 0 mV). The ensemble *I–V* curves present data from neurons with a dominant fast-inactivating component ($n = 49$; top) and from neurons with only slow-inactivating components ($n = 35$; bottom). Note that the fast-inactivating component had a lower threshold. ***D***, Physiological separation of fast- and slow-inactivating components. The superimposed traces show consecutive current records for the effect of a 0.5 s, −20 mV prepulse in removing the fast-inactivating component. ***E***, Ca^{2+}-dependent inactivation of $I_{Ba(Ca)}$. Superimposed current traces from consecutive records of the same cell demonstrate that fast inactivation of $I_{Ba(Ca)}$ did not occur in Ca^{2+}-free solution. ***F***, Removal of $I_{Ba(Ca)}$ by 0.2 mM Cd^{2+} in neurons with different decay kinetics. Neurons displaying fast- or slow-inactivating component were represented by filled or open symbols, respectively. Vertical calibration bars: 100 pA or 25 mV. Horizontal calibration bars: 100 ms for voltage-clamp traces and 50 ms for current-clamp traces. Standard bath solution was composed of the following (in mM): 128 NaCl, 2 KCl, 4 $MgCl_2$, 1.8 $CaCl_2$, and 35.5 sucrose, buffered at pH 7.1 with 5 HEPES.

served broadened spikes, sometimes followed by plateau potentials, reflecting the balancing acts of the modified depolarization and repolarization forces after Ba^{2+} treatments.

To improve isolation of currents flowing through Ca^{2+} channels, Ba^{2+} (20 mM), in addition to Ca^{2+} (1.8 mM), was used along with Na^+ and K^+ channel blockers (10 nM TTX, 1 mM 4-AP, 2.5 mM TEA, and 50 μM quinidine) in standard bath solution, in conjunction with K^+-free (replaced by Cs^+) pipette solution. After growing 2 d in culture, most WT neurons (~80%; $n = 104$) expressed an inward current [termed $I_{Ba(Ca)}$]. Two types of $I_{Ba(Ca)}$ were classified in the neuronal populations based on their distinct decay kinetics (τ of $<$100 vs $>$300 ms for the major decay component) (Fig. 1*C*). The current–voltage (*I–V*) relationships show that both types of inward currents reach their maximum at ~0 mV. However, the fast-inactivating current was activated at more negative potentials than the slow-inactivating component (approximately −40 vs −20 mV) (Fig. 1*C*). Some cells expressed both fast- and slow-inactivating currents, which could be isolated by using a prepulse inactivation protocol (Fig. 1*D*). These properties of Ca^{2+} currents are consistent with previous single-channel and whole-cell studies on other *Drosophila* neuronal culture systems (Leung et al., 1989; Leung and Byerly, 1991; Schmidt et al., 2000).

Ba^{2+} is also known to suppress Ca^{2+}-dependent inactivation of Ca^{2+} channels (Hille, 2001). Consistently, we found that, in Ca^{2+}-free, Ba^{2+}-containing saline (20 mM), neurons no longer displayed fast inactivation ($n = 67$). Adding a physiological concentration of Ca^{2+} (1.8 mM) restored inactivation of the inward currents (mean ± SEM, τ_{0Ca}, 267 ± 17 ms vs $\tau_{1.8Ca}$, 86 ± 27 ms; $n = 5$; $p < 0.005$, paired *t* test) (Fig. 1*E*). The amplitude of inward current was proportional to the external concentration of Ba^{2+} (5–20 mM; data not shown). Therefore, throughout the remaining study, the bath solution contained 20 mM Ba^{2+} and 1.8 mM Ca^{2+}, in addition to Na^+ and K^+ channel blockers, for characterizing *cac* channel-mediated currents, with the resultant currents termed $I_{Ba(Ca)}$. Notably, a general Ca^{2+} channel blocker Cd^{2+} (0.2 mM) was capable of blocking both types of $I_{Ba(Ca)}$ (Fig. 1*F*).

Removal of a major component of neuronal Ca^{2+} currents by *cac* mutations

Neuronal currents mediated by *cac* channels have not been characterized under voltage-clamp conditions. We compared record-

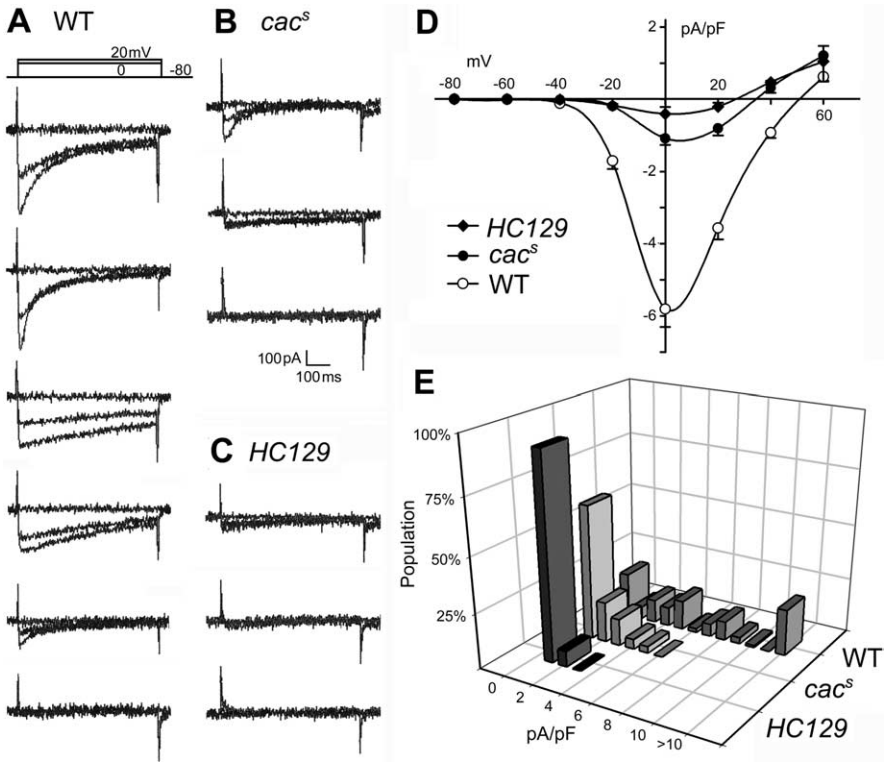

Figure 2. Neuronal Ca^{2+} channels encoded by *cac*. ***A***, Representative traces from six WT neurons with different $I_{Ba(Ca)}$ density and kinetics. Neurons with no detectable $I_{Ba(Ca)}$ were rare (bottom). ***B***, Strong reduction of $I_{Ba(Ca)}$ in cac^s mutant neurons. The remaining $I_{Ba(Ca)}$ still displayed fast- or slow-inactivation kinetics. Neurons without detectable $I_{Ba(Ca)}$ were frequently encountered. ***C***, Near elimination of $I_{Ba(Ca)}$ in neurons of $l(1)L13^{HC129}$ deficiency line. Most neurons from this line produced no detectable $I_{Ba(Ca)}$. ***D***, *I–V* relationships for peak $I_{Ba(Ca)}$ from different genotypes [$n = 104$, 65, and 25 for WT, cac^s, and $l(1)L13^{HC129}$]. ***E***, Histograms of $I_{Ba(Ca)}$ density at 0 mV. Note abundance of neurons without detectable $I_{Ba(Ca)}$ in both cac^s and $l(1)L13^{HC129}$ cultures.

channels that are responsible for operating major Ca^{2+} currents of different activation voltages and inactivation kinetics in *Drosophila* neurons.

Current-clamp experiments effectively revealed the contribution to neuronal depolarization by *cac*-mediated currents of different amplitudes, kinetics, and voltage dependence. Consecutive voltage- and current-clamp recordings were performed on the same cells to investigate the rising phase and maintenance of membrane depolarization. In the presence of TTX, $I_{Ba(Ca)}$ was the remaining depolarizing force. During depolarizing current injection, neurons with substantial $I_{Ba(Ca)}$ generated all-or-none, regenerative activities (Ca^{2+} spikes or action potentials) (Fig. 3*A*, first two cells). After spike initiation, the membrane potential remained depolarized, outlasting current injection, as a result of Ba^{2+} inhibition of Ca^{2+} channel inactivation and reduced repolarization by K^+ channel blockers in the saline. In contrast, neurons lacking detectable $I_{Ba(Ca)}$ exhibited typical passive membrane responses (Fig. 3*A*, last cell). The threshold levels for Ca^{2+} spikes, as indicated by the inflection point, differed between neurons that exhibited fast- and slow-inactivating $I_{Ba(Ca)}$ [mean ± SEM (*n*), −13.8 ± 1.4 mV (12) vs −7.0 ± 1.5 mV (9); $p < 0.01$]. This also reflects differences in activation voltages of the two currents (compare with Fig. 1*C*).

In *cac* cultures, the proportion of neurons unable to generate Ca^{2+} spikes was drastically increased (for representative traces, see Fig. 3*B*,*C*). Only a few cac^s neurons expressed small but detectable $I_{Ba(Ca)}$ (Fig. 2*B*,*E*), and their associated action potentials displayed a slow rise (dV/dt in volts per second) (Fig. 3*D*). Note that the maximum rise occurred at the time of inflection point of Ca^{2+} spikes of the corresponding traces, as indicated by symbols (Fig. 3*A*,*B*,*D*). Once evoked, the thresholds of Ca^{2+} spikes in *cac* neurons [−11.7 ± 1.7 (4) vs −6.2 ± 0.9 (4) for cells with fast- vs slow-inactivating $I_{Ba(Ca)}$] were not significantly different from those in WT.

ings from neurons dissociated from WT and *cac* mutant alleles. As described above, neurons in WT cultures expressed varying amplitudes and kinetics of $I_{Ba(Ca)}$ (Figs. 1*B*, 2*A*), and, in some neurons, $I_{Ba(Ca)}$ was not detectable (<1 pA/pF) (Fig. 2*A*). The extent of variability is shown in the amplitude histogram (Fig. 2*E*). In cultures of cac^s, a hypomorph, $I_{Ba(Ca)}$ was drastically reduced (Fig. 2*B*). The *I–V* curves for the peak $I_{Ba(Ca)}$ current (Fig. 2*D*) show that, on average, $I_{Ba(Ca)}$ in cac^s cultures was less than one-fifth in amplitude of that in WT. Notably, the residual currents in *cac* neurons still displayed both fast- and slow-inactivating components (Fig. 2*B*), but the proportion of neurons with no detectable $I_{Ba(Ca)}$ was greatly increased from 20% in WT to >50% in cac^s (Fig. 2*E*). To rule out the possibility of undesirable genetic background contributions, we examined another independently isolated allele cac^{ts2}. The results demonstrate that cac^{ts2} mutation also affects both fast- and slow-inactivating Ca currents (data not shown). On average, $I_{Ba(Ca)}$ in cac^{ts2} cultures was significantly reduced [mean ± SEM (*n*), WT, −5.61 ± 0.50 pA/pF (104) vs cac^{ts2}, −1.78 ± 0.46 pA/pF (18); $p < 0.005$, *t* test].

The use of embryonic cultures also allowed studies of lethal mutations. Single-embryo cultures of homozygous deficiency $l(1)L13^{HC129}$ could be identified by the absence of green fluorescent protein (GFP) signal, because the stock was maintained over a marked balancer chromosome, *FM7, P{w*$^{+mC}$ *= Act GFP}* (Kawasaki et al., 2002). In homozygous cultures, >90% of neurons produced no detectable $I_{Ba(Ca)}$ (Fig. 2*C*,*E*). $I_{Ba(Ca)}$ in this deficiency mutant was much smaller than that found in cac^s (Fig. 2*D*). Our mutational analysis demonstrates that *cac* encodes the

Sensitivity of neuronal Ca^{2+} channels to T- and L-type channel blockers

The sensitivities of vertebrate Ca^{2+} channels to specific pharmacological agents correspond well to their molecular classifications (Ertel et al., 2000). We characterized the sensitivity of *Drosophila* neuronal $I_{Ba(Ca)}$ with several blockers commonly used for vertebrate Ca^{2+} channel identification. Vertebrate T-type channels are characterized by a low threshold of activation and fast inactivation compared with L-type channels. As shown above, Cd^{2+} that blocks both T- and L-type channels could also remove most of the *Drosophila* neuronal $I_{Ba(Ca)}$, regardless of the decay kinetics (Fig. 1*F*). Unexpectedly, two T-type Ca^{2+} channel blockers, amiloride (1 mM) and Ni^{2+} (0.1–0.2 mM), blocked not only the low-threshold, fast-inactivating $I_{Ba(Ca)}$ but also the high-threshold, slow-inactivating $I_{Ba(Ca)}$ (Fig. 4*A*,*B*). In contrast, two L-type channel blockers, nifedipine (10 μM) and diltiazem (0.5

mM), had little effect on either type of $I_{Ba(Ca)}$ (Fig. 4*A*,*B*). In fly muscles, it has been shown that the Ca^{2+} currents are sensitive to L-type rather than T-type blockers (Gielow et al., 1995). Together, the results indicate distinct pharmacological profiles for the dominant Ca^{2+} currents in neurons and muscles.

We further tested T- and L-type channel blockers on WT and *cac* neurons for Ca^{2+} spike generation. Although the drug effect on the small residual $I_{Ba(Ca)}$ in *cac* neurons was difficult to quantify with voltage clamping, current-clamp recordings effectively detected the weakening of Ca^{2+} spikes during drug treatment. In WT cultures, nifedipine treatments had little effects ($n = 5$) (Fig. 4*C*), but either amiloride or Ni^{2+} application slowed down the rising phase of Ca^{2+} spikes ($n = 4$ and 4, respectively) (for sequential applications on the same cell, see Fig. 4*C*). These data are consistent with the results from voltage-clamp studies (Fig. 4*A*,*B*). The Ca^{2+} spikes in *cac*^{s} cultures were also resistant to nifedipine ($n = 4$; data not shown). However, unlike the clear blocking effect in WT, amiloride and Ni^{2+} treatments did not alter the rising phase of Ca^{2+} spikes in some *cac*^{s} neurons (Ni^{2+}, 3 of 7; amiloride, 2 of 4) (Fig. 4*D*). Therefore, in *cac*^{s} neurons insensitive to Ni^{2+} and amiloride, the remaining $I_{Ba(Ca)}$ may be mediated by either *cac* channels with genetically modified pharmacological sensitivity or non-*cac* channels.

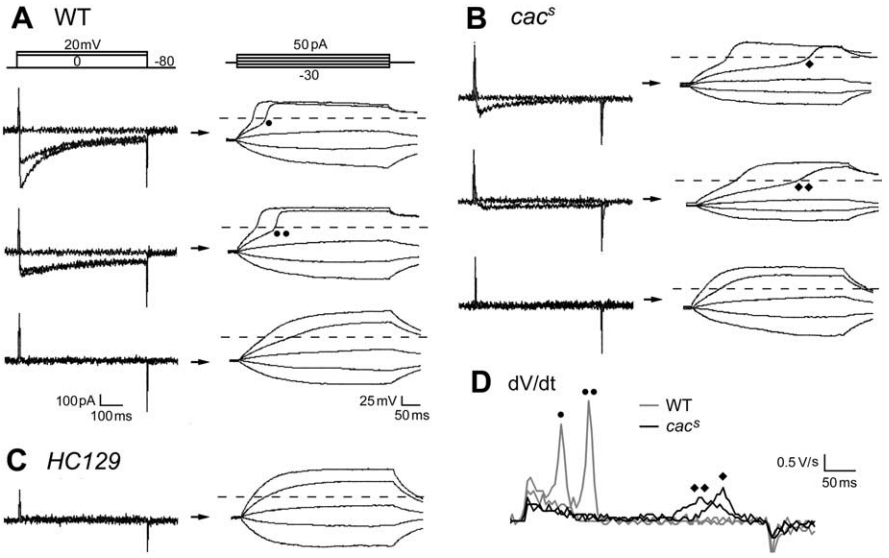

Figure 3. Weakened regenerative potentials in *cac* neurons. ***A***, Relationships of inward currents and regenerative potentials in WT neurons. In addition to 20 mM Ba^{2+}, TTX and K^+ channel blockers (Fig. 1 legend) were present in standard bath solution. Therefore, the inward currents and regenerative potentials sequentially recorded from the same cells reflected Ca^{2+} channel activity. Note the inflection points at which the regenerative potential was initiated. Depolarization of neurons with $I_{Ba(Ca)}$ reached a plateau level, which is determined by the equilibrium potential of the inward current and is independent of additional increase of current injection. In neurons lacking detectable $I_{Ba(Ca)}$ (bottom), membrane polarization was proportional to the amount of current injected, following the kinetics determined by passive membrane properties. Dash lines indicate 0 mV. ***B***, ***C***, Weakened regenerative potentials associated with decreased $I_{Ba(Ca)}$ in *cac* mutant neurons. ***D***, Reduced rate of depolarization (dV/dt) during initiation of regenerative potentials in *cac* mutant neurons. The corresponding rate of membrane potential change of the selected traces in ***A*** and ***B*** are indicated by circles and diamonds next to the inflection point, around which maximum dV/dt occurs.

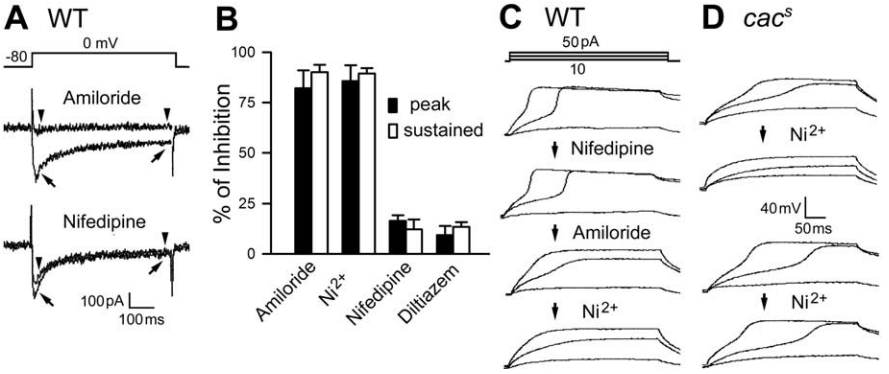

Figure 4. Sensitivity of *Drosophila* neuronal Ca^{2+} channels to T-type channel blockers. Two T-type channel blockers, amiloride (1 mM) and Ni^{2+} (0.1 mM), and two L-type channel blockers, nifedipine (10 μM) and diltiazem (0.5 mM), were examined. ***A***, Superimposed current traces obtained before (arrows) and after (arrowheads) amiloride and nifedipine treatments in WT neurons. ***B***, Percentage of $I_{Ba(Ca)}$ inhibition by different drugs in WT neurons. Reduction in both peak and sustained components (measured at the times indicated by arrows and arrowheads in ***A***) indicates that both fast- and slow-inactivating components of Ca^{2+} currents were sensitive to amiloride and Ni^{2+} ($n = 6$ and 7, respectively). In contrast, nifedipine and diltiazem removed <20% of the $I_{Ba(Ca)}$ ($n = 6$ and 5, respectively). ***C***, ***D***, Different drug effects on regenerative membrane potentials in WT and *cac* neurons. Nifedipine exerted little effect, but amiloride and Ni^{2+} progressively removed regenerative potentials in WT neurons (an example of sequential recording shown in ***C***). In contrast, only some *cac*^{s} neurons examined were sensitive to Ni^{2+} (4 of 7; top in ***D***) and amiloride (2 of 4), but the remaining samples were unaffected by either Ni^{2+} (bottom) or amiloride.

Reduction of Ca^{2+}-activated K^+ currents in *cac* neurons

The dynamic regulation of intracellular Ca^{2+} is known to affect a wide range of molecular, cellular, and developmental events. One immediate target is Ca^{2+}-activated $I_{K(Ca)}$ channels, which serve as a feedback mechanism for membrane repolarization and termination of voltage-dependent Ca^{2+} influx. We investigated how the suppression of Ca^{2+} influx in *cac* neurons affects $I_{K(Ca)}$ by using Ba^{2+}-free (1.8 mM Ca^{2+}), TTX-containing bath solution and Cs^+-free pipette solution [to compare with standard saline for $I_{Ba(Ca)}$ measurement, see Materials and Methods]. After Cd^{2+} application, $I_{K(Ca)}$ was extracted by subtracting the remaining outward current from the total current before Cd^{2+} treatment (Singh and Wu, 1989; Saito and Wu, 1991). In this procedure, contamination from inward I_{Ca} was negligible because of its small size (<50 vs >1000 pA for outward currents) (compare Figs. 1*A*, 5*A*). The small Ca^{2+} influx sufficient for activating $I_{K(Ca)}$ is consistent with the high-affinity $I_{K(Ca)}$ channels in *Drosophila* (submicromolar Ca^{2+}) (Komatsu et al., 1990). The extracted $I_{K(Ca)}$ from WT neurons was variable in current kinetics and size (Fig. 5*A*,*E*). WT neurons could express either or both of the transient and sustained components of $I_{K(Ca)}$ (Fig. 5*A*) (cf. Saito and Wu, 1991). The peak current density of $I_{K(Ca)}$ ranged from 1 to 40 pA/pF during depolarization to +60 from −80 mV. Because amiloride was also effective in blocking Ca^{2+} currents (1 mM) (Figs. 1, 4), amiloride-sensitive K^+ currents were also determined as another measure for $I_{K(Ca)}$. As expected, Cd^{2+}- and amiloride-sensitive K^+ currents shared similar *I–V* relationships (Fig. 5*D*) and a similarly wide range of current densities (Fig. 5*E*). Adding amiloride after Cd^{2+}, or

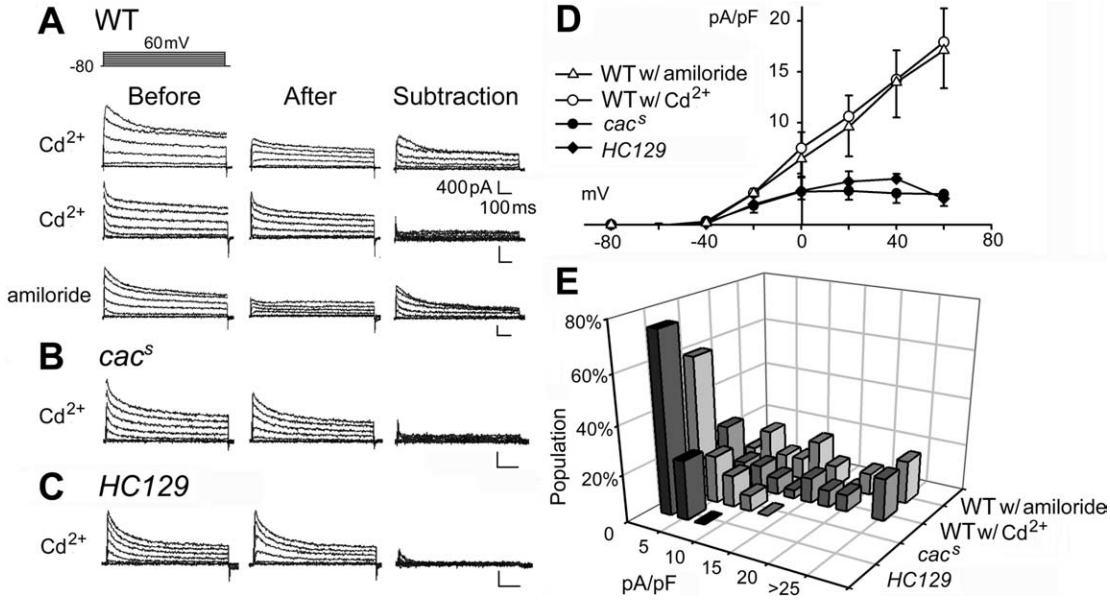

Figure 5. Severe reduction of Ca^{2+}-activated K^+ currents [$I_{K(Ca)}$] in *cac* neurons. $I_{K(Ca)}$ was extracted from subtracting Cd^{2+}-sensitive currents from total outward current in standard bath saline, in which Cd^{2+} (0.2 mM) was added to eliminate Ca^{2+}-dependent currents. The difference in current amplitude before and after Cd^{2+} treatment yields $I_{K(Ca)}$ with a minimal contamination of I_{Ca} (<5%; compare with Fig. 1*A*). ***A***, $I_{K(Ca)}$ in WT cultures. Most WT neurons (>60%) produced large $I_{K(Ca)}$ (>6 pA/pF) with a minority displaying little $I_{K(Ca)}$. Application of amiloride to block *cac* channels produced similar estimates of $I_{K(Ca)}$. ***B***, ***C***, Strong suppression of $I_{K(Ca)}$ in cac^s and $l(1)L13^{HC129}$ mutant cultures. ***D***, Ensemble *I–V* curves demonstrating strong suppression of $I_{K(Ca)}$ in *cac* mutant cultures. Note that estimation of $I_{K(Ca)}$ based on extraction of amiloride-sensitive K^+ currents in WT neurons produced results similar to Cd^{2+}-sensitive K^+ currents. ***E***, Histograms of $I_{K(Ca)}$ amplitude distribution. Note the similarities between $I_{K(Ca)}$ and $I_{Ba(Ca)}$ density distributions for WT as well as *cac* mutant alleles (compare with Fig. 2*E*). Sample sizes, $n = 28$, 8, 19, and 10 for WT with Cd^{2+}, WT with amiloride, cac^s, and $l(1)L13^{HC129}$.

the other way around, did not further reduce the K^+ current amplitude (data not shown).

In contrast, most neurons from the two *cac* alleles carried little detectable $I_{K(Ca)}$ (<2 pA/pF) (Fig. 5*B*,*C*,*E*). Among the few *cac* neurons that expressed detectable $I_{K(Ca)}$, the current density was rarely beyond 10 pA/pF (Fig. 5*E*). The percentage of cac^s neurons carrying $I_{K(Ca)}$ was directly comparable with that of neurons expressing $I_{Ba(Ca)}$ (~20%) (Figs. 2*E*, 5*E*). Moreover, $I_{K(Ca)}$ and $I_{Ba(Ca)}$ reduction in the *cac* mutants was similar in profiles (Figs. 2*D*, 5*D*). These results suggest that neuronal Ca^{2+} influx through *cac* channels provides a major source of Ca^{2+} for $I_{K(Ca)}$ activation.

Homeostatic upregulation of inactivating I_A in *cac* neurons

Voltage-activated K^+ currents are activated in response to membrane depolarization. After removal of inward I_{Ca} and outward $I_{K(Ca)}$ by Cd^{2+}, the remaining outward currents contained two distinct voltage-activated components, inactivating I_A and noninactivating I_K, which can be separated by a prepulse inactivation protocol (Zhao and Wu, 1997; Yao and Wu, 1999, 2001; Peng and Wu, 2007). We found in cac^s cultures that I_A was unexpectedly upregulated, whereas I_K was unaltered (Fig. 6*A*,*B*,*D*).

Interestingly, I_A increase in *cac* neurons can be phenocopied by WT neurons after chronic pharmacological blockade of *cac* Ca^{2+} channels (Fig. 6*D*). Ni^{2+} (0.05 mM) was applied to WT cultures throughout the culture lifespan (2–3 d). Before recording, Ni^{2+} was washed out, and $I_{K(Ca)}$, I_A, and I_K were isolated by application of Cd^{2+} and the prepulse protocol sequentially. Ni^{2+} treatment decreased $I_{K(Ca)}$ and, at the same time, increased I_A without altering I_K (Fig. 6*D*). These changes in current density were significant but to a lesser extent compared with the modifications in cac^s neurons.

In contrast, short-term Ni^{2+} treatments (15–20 min) did not cause any detectable alterations in $I_{K(Ca)}$, I_A, I_K (Fig. 6*C*,*D*), and $I_{Ba(Ca)}$ (data not shown). Short-term treatment of another *cac* channel blocker, amiloride (1 mM), did not result in detectable changes in K^+ currents either, suggesting that the K^+ current upregulation requires a relatively slow process. [Long-term incubation with amiloride was not attempted because amiloride is light sensitive (Gielow et al., 1995) and the resultant products appeared to be toxic to cultured neurons.] Remarkably, the size of I_A increase in *cac* neurons as well as in chronically Ni^{2+}-treated WT cultures approximately matched the degree of $I_{K(Ca)}$ reduction (Fig. 6*D*), resulting in no appreciable changes in total outward K^+ currents (Fig. 6*E*).

It is known that posttranslational modifications such as phosphorylation affect channel properties, including voltage dependence and kinetics of channel activation and inactivation (Jonas and Kaczmarek, 1996; Yao and Wu, 2001). To investigate whether upregulated I_A in *cac* neurons displays obvious signs of modified properties indicating channel posttranslational modifications, we examined the parameters including voltage of half steady-state inactivation ($V_{1/2}$), kinetics of decay (τ), and recovery from inactivation ($t_{1/2}$). We did not detect any significant differences in these properties of I_A between WT and *cac* cultures (Fig. 6*F*), despite the striking amplitude increase in *cac* neurons. These results do not support the possibility of posttranslational modifications of I_A channels caused by *cac* mutations.

mRNA levels of K^+ channel genes in *cac* mutants

In *Drosophila*, *Shaker* (*Sh*) and *Shal* encode I_A channels, whereas *slowpoke* (*slo*) and SK code for $I_{K(Ca)}$ channels (Jan et al., 1977; Tanouye et al., 1981; Wei et al., 1990; Atkinson et al., 1991; Adelman et al., 1992). To determine whether transcriptional modifications of these identified genes could be responsible for the altered K^+ current expression observed in *cac* mutants, we quantified their mRNA levels in adult heads by performing RT-PCR.

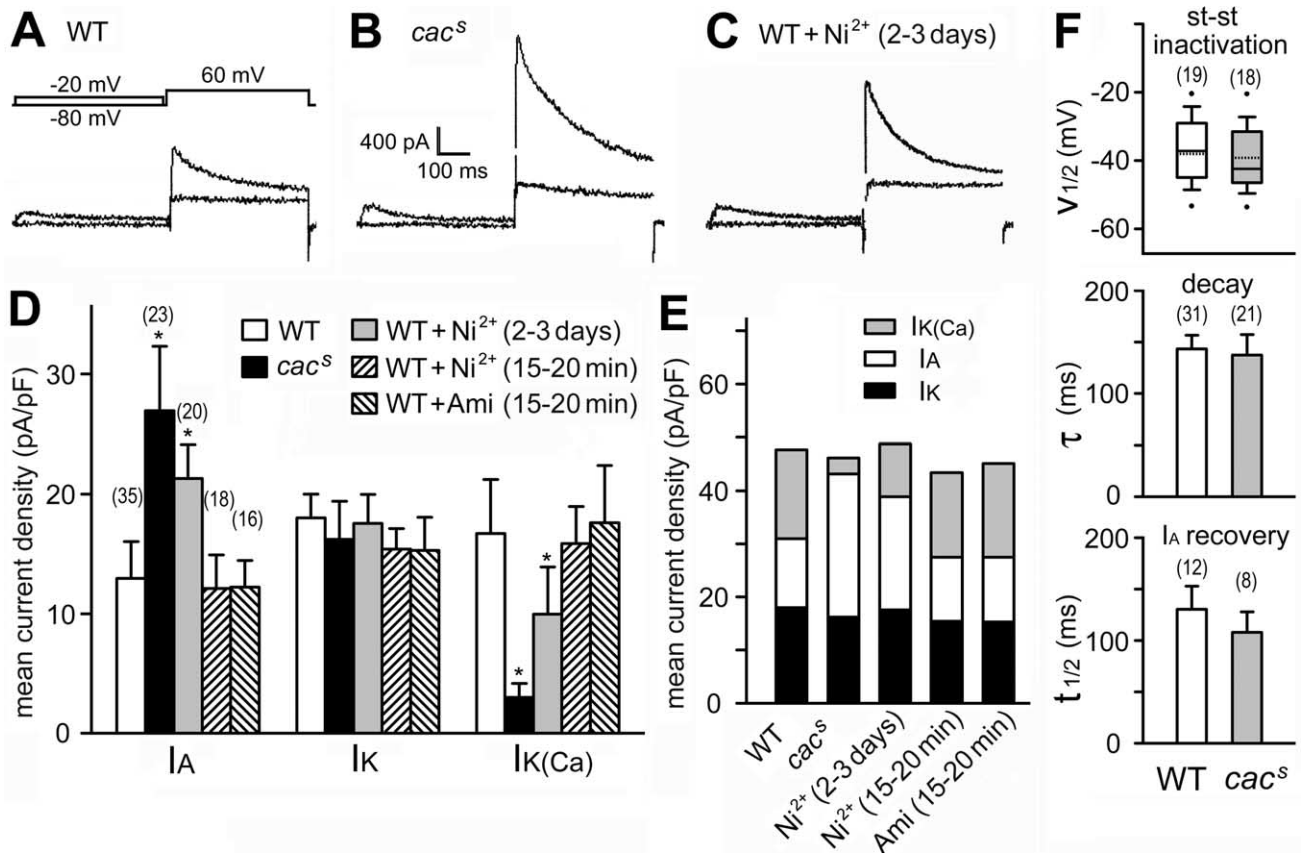

Figure 6. Homeostatic upregulation of voltage-dependent I_A in *cac* neurons. ***A–C***, Separation of transient I_A and sustained I_K by a prepulse protocol after removal of Ca^{2+}-dependent currents by Cd^{2+}. Representative traces demonstrate a substantial I_A increase in cac^s neurons compared with WT neurons. WT neurons pretreated with the *cac* channel blocker Ni^{2+} (0.05 mM) for 3 d phenocopied upregulation of I_A observed in *cac* neurons. ***D***, Mean current densities for extracted I_A, I_K, and $I_{K(Ca)}$. Note upregulation in I_A but not I_K in cac^s neurons and WT neurons with chronic blockade (2–3 d) of *cac* channels. However, short-term blockade (15–20 min) of *cac* channels by Ni^{2+} or amiloride (0.5 mM) did not alter current densities. $*p < 0.05$ against WT, one-way ANOVA. ***E***, Summation of I_A, I_K, and $I_{K(Ca)}$ among neurons of different genotypes or with drug treatments. Note the similar total K^+ currents, which suggest a homeostatic, compensatory increase of I_A for reduction of $I_{K(Ca)}$. ***F***, Properties of upregulated I_A in *cac* neurons compared with WT I_A. Steady-state (st-st) inactivation of I_A is compared for $V_{1/2}$, at which half-inactivation is attained. Solid and dashed lines in the box plots indicate median and mean values. Decay time constant (τ) was determined at +60 mV. Half-time ($t_{1/2}$) of I_A recovery from inactivation was determined with a twin-pulse (+20 mV) protocol with varying interpulse intervals. Data indicate no significant differences in these biophysical parameters. Error bars represent SEM with sample sizes indicated.

The amplification rate during RT-PCR cycles gave an estimate of the abundance of individual K^+ channel transcripts (Fig. 7).

Our RT-PCR results from adult heads showed only slight but statistically insignificant decrease in *slo* and *SK* mRNA in *cac* mutants (Fig. 7*B*), although electrophysiological results from embryonic neuronal cultures demonstrate a drastic $I_{K(Ca)}$ reduction in *cac* cultures (Fig. 5). These results support the idea of a normal density of $I_{K(Ca)}$ channels with deprived activity attributable to insufficient I_{Ca} in *cac* neurons. Unlike *slo* and *SK* mRNAs, we detected a significant increase of *Sh* mRNA levels in *cac* mutants (42%) (Fig. 7*A*,*B*). The data suggest that a modification at the mRNA level may be a contributing factor for the increase of I_A in *cac* cultures. Apparently, *Sh* was preferentially upregulated because *Shal* mRNA levels were not increased.

Unaltered Ca^{2+} current density in K^+ channel mutants

The above results demonstrate an important role of *cac* Ca^{2+} channels in the long- and short-term regulations of neuronal K^+ currents (Figs. 5, 6). It would be of interest to determine whether K^+ channel mutations could in turn affect Ca^{2+} current expression. We measured $I_{Ba(Ca)}$ in neurons dissociated from *Sh*, *Shab* (Singh and Singh, 1999), and *slo* mutants, which lack voltage-gated inactivating, non-inactivating, and Ca^{2+}-gated K^+ chan-

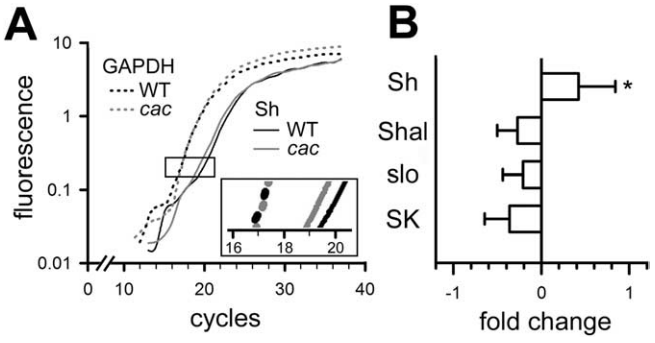

Figure 7. Determination of mRNA abundance for K^+ channels in WT and *cac* neurons by RT-PCR. ***A***, Amplification rates of *GAPDH* and *Sh* transcripts from WT and *cac* fly heads based on the accumulation of fluorescence intensity throughout PCR cycles. Inset, Enlargement for the segment between cycles 16 and 20. The rate for the *Sh* fragment in *cac* mutants was faster than that in WT, but the rate for the control *GAPDH* fragment was nearly identical for the two genotypes. ***B***, Differences in transcript abundance of *Sh* and *Shal* I_A channels and of *slo* and *SK* $I_{K(Ca)}$ channels between WT and *cac*. The mRNA levels for individual K^+ channel genes are estimated by the fluorescence change normalized to *GAPDH* control. The positive value in the bar graph indicates an increase in RNA abundance in *cac* over WT. Data from three independent RNA purifications. Error bars indicate SD. $*p < 0.05$, two-way ANOVA for genotype and channel subtype comparisons.

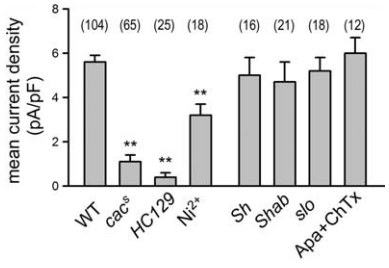

Figure 8. Lack of modifications in Ca^{2+} channel-mediated currents in K^+ channel mutants. Mean $I_{Ba(Ca)}$ densities among neurons in *cac* and Ni^{2+}-treated WT cultures are compared with cultures of K^+ channel mutants. Sh^M, with altered I_A, $Shab^3$, with defective to I_K, slo^1, with defective to $I_{K(Ca)}$. No modifications of $I_{Ba(Ca)}$ densities were found in K^+ channel mutant neurons and in WT neurons with chronic blockade (2–3 d) of Ca^{2+}-activated K^+ channels by 5 μM apamine and 50 nM charybdotoxin (Apa + ChTx). Error bars represent SEM with sample sizes indicated. $^{**}p < 0.005$ against WT control, one-way ANOVA.

nels, respectively. Among the null or nearly null mutant alleles examined (Sh^M, $Shab^3$, and slo^1) (Jan et al., 1977; Tanouye et al., 1981; Elkins et al., 1986; Wei et al., 1990; Singh and Singh, 1999), we did not detect any significant alterations in $I_{Ba(Ca)}$ amplitude (Fig. 8). Furthermore, prolonged incubation (2 d) of WT neurons with two $I_{K(Ca)}$ blockers, apamine (5 μM) and charybdotoxin (50 nM), did not affect the densities of $I_{Ba(Ca)}$. These results indicate a central role of *cac* Ca^{2+} channels in neuronal homeostatic regulation; manipulations of Ca^{2+} influx through *cac* channels strongly affect K^+ current expression, whereas elimination of individual K^+ channels is not sufficient to cause homeostatic changes in Ca^{2+} channels.

Discussion

Short- versus long-term regulations of K^+ currents by *cac* channel-mediated Ca^{2+} currents

Intracellular Ca^{2+} is critical for regulation of neuronal membrane excitability and neurotransmission. In excitable cells, intracellular Ca^{2+} triggers Ca^{2+}-activated $I_{K(Ca)}$, which contributes to repolarization of action potential and the subsequent hyperpolarizing after potential (for review, see McManus, 1991; Vergara et al., 1998). In the giant neuron culture of *Drosophila*, we confirmed the tight functional coupling between *cac*-mediated Ca^{2+} current and $I_{K(Ca)}$, as indicated by a same proportion of cac^s neurons that expressed $I_{Ba(Ca)}$ and $I_{K(Ca)}$ (both ~20%) and by a similar extent of reduction in the two currents (Figs. 2, 5). The result reflects a unidirectional functional dependence, because the Ca^{2+} current amplitude is not affected by the $I_{K(Ca)}$ mutation *slo* or by chronic treatment with $I_{K(Ca)}$ blockers (Fig. 8).

A number of potential mechanisms could be responsible for the I_A upregulation observed in *cac* mutant neurons (Fig. 6), including transcriptional, translational, and posttranslational modifications. Posttranslational modifications by Ca^{2+}-dependent protein kinase phosphorylation and dephosphorylation can substantially change K^+ channel activities and properties within tens of seconds to minutes (Jonas and Kaczmarek, 1996; Wicher et al., 2001). Such posttranslational modulation of K^+ currents is known to underlie activity-dependent plasticity of synaptic transmission in molluscan species (Byrne and Kandel, 1996; Alkon, 1999) and is altered in *Drosophila* cAMP pathway mutants defective in memory processes (Zhong and Wu, 1993; Wright and Zhong, 1995). *Drosophila Sh* channels are modified by cAMP-dependent modulation in a heterologous expression system (Drain et al., 1994) and in larval muscles (Zhong and Wu, 1993) as well as in embryonic and larval cultured neurons (Wright and Zhong, 1995; Yao and Wu, 2001). We examined properties of the upregulated I_A in *cac* or pharmacologically treated WT cultures (Fig. 6) for indications of I_A modulation. However, our results did not provide any compelling evidence for channel modulation. Furthermore, the homeostatic regulation observed requires long-term blockade of *cac* channels (days instead of minutes) (Fig. 6), beyond the ordinary timescale of modulation by protein kinases.

In contrast to the above short-term regulations, there are also long-term Ca^{2+}-dependent effects on neuronal differentiation, growth, and plasticity, in which protein synthesis or gene expression is required. For example, when neuronal spike activity is manipulated, a homeostatic regulation is initiated, in which the activity-dependent intracellular Ca^{2+} accumulation induces compensatory excitability changes by adjusting the relative abundance of ion channels (Spitzer, 1999; Turrigiano, 1999). In *Xenopus* embryonic cultures, changing the timing of Na^+ channel expression or pharmacologically suppressing Na^+ or Ca^{2+} channel function alters the subsequent developmental time course of K^+ current (O'Dowd et al., 1988; Linsdell and Moody, 1994, 1995). In addition, overexpression of Shal I_A in lobster neurons triggers a compensatory increase of hyperpolarization-activated inward I_h (MacLean et al., 2003). Our study presents a case of homeostatic regulation of voltage-dependent K^+ currents by genetic manipulation of *cac* channel-mediated Ca^{2+} currents in *Drosophila*. In *cac* neuronal cultures, a significant increase was observed in voltage-activated I_A but not I_K, an upregulation that could be mimicked by chronic blockade of *cac* channels in WT cultures (Fig. 6). The lack of $I_{K(Ca)}$ in *cac* neurons appeared to be compensated by an increase in I_A, and consequently the total outward K^+ currents remained essentially unaltered (Figs. 5, 6).

It has been demonstrated in identified neurons that transcript numbers of several types of K^+ channels correspond to their current sizes in crustacean species (Baro et al., 1997; Schulz et al., 2006). In microarray experiments, *Drosophila* mutations affecting neuronal excitability and nerve terminal development can lead to upregulation or downregulation of ion channel and receptor RNA levels (Guan et al., 2005). Increase in synaptic input levels by genetic manipulations could decrease transcript numbers of the *para* (*paralytic*) Na^+ channels in identified *Drosophila* motor neurons (Mee et al., 2004). Furthermore, the mRNA level of *slo* BK (large-conductance calcium-activated) channels is sensitive to behavior conditioning, strongly upregulated after alcohol sedation (Cowmeadow et al., 2006). In *Drosophila* giant neuron cultures, *Shab* mutant neurons, defective in slow-inactivating K^+ currents, show an upregulation of fast-inactivating K^+ currents (Peng and Wu, 2007). In the current study, an upregulation of I_A was also observed in *cac* mutant neurons (Fig. 6). Our quantitative RT-PCR studies on adult brain tissue indicate a 40% increase in *Sh* mRNA levels in *cac* mutants (Fig. 7). Such results are consistent with the idea that a mechanism at the RNA level contributes to the observed homeostatic upregulation of I_A in embryonic neuronal cultures (Fig. 6) and suggest the possibility that I_A is upregulated in adult *cac* neurons as well. It is worth noting that *Shal* mRNA level was not altered in *cac* neurons, although *Shal*, rather than *Sh*, channels are considered to be the dominant contributor to I_A in the neuronal soma (Baker and Salkoff, 1990; Baro et al., 1997; Gasque et al., 2005; Peng and Wu, 2007). These data suggest an interesting possibility that *Sh* plays a role in neuronal plasticity for upregulation and downregulation of neuronal excitability during environmental challenges or behavioral conditioning. It has been shown that Sh mutations affect learning in a courtship conditioning paradigm and a non-associative habituation paradigm (Cowan and Siegel, 1984; Engel and Wu, 1998).

Major Ca^{2+} currents in *Drosophila* neurons encoded by the *cac* gene

In vertebrate nervous systems, low-threshold, fast-inactivating T type Ca^{2+} channels coexist with high-threshold, slow-inactivating L-, N-, P-, and Q-type Ca^{2+} channels (Hille, 2001). Molecular characterizations have revealed that these channels are encoded by separate genes, and their differential expression leads to different patterns of intracellular Ca^{2+} dynamics. In *Drosophila*, studies of dissociated embryonic neurons demonstrated two distinct components of Ca^{2+} currents, which parallel the vertebrate low-threshold, fast-inactivating and high-threshold, slow-inactivating Ca^{2+} currents (Figs. 1, 2) (Byerly and Leung, 1988; Saito and Wu, 1991; Schmidt et al., 2000). The two components can also be distinguished pharmacologically (Leung et al., 1991). Nevertheless, our study suggests that the *cac* channels mediate a major Ca^{2+} currents in *Drosophila* embryonic neurons, because *cac* deficiency, $l(1)L13^{HC129}$, nearly eliminates both fast- and slow-inactivating Ca^{2+} currents in our soma recording (Fig. 2). This conclusion is also supported by the observation that both components in WT were inhibited by vertebrate T-type channel blockers (Fig. 4). However, a minor component of Ca^{2+} current still remained in the *cac* deficiency mutant, implying a role of *Dmca1D* or other unidentified genes in neuronal Ca^{2+}-dependent functions. It remains to be investigated, in neurons at the larval, pupal, and adult stages, to what extent Ca^{2+} currents are reduced and whether both fast- and slow-inactivating Ca^{2+} currents are affected by *cac* mutations.

Deletion of either *Dmca1D* or *cac*, two known Ca^{2+} channel genes in *Drosophila*, causes lethality, suggesting that their roles in the organism are not redundant (Smith et al., 1996; Eberl et al., 1998). Genetic, electrophysiological, and pharmacological experiments have demonstrated that *Drosophila* muscle Ca^{2+} currents consist of a major, DHP-sensitive and a minor, amiloride-sensitive component (D- and A-currents, respectively) (Gielow et al., 1995; Ren et al., 1998). In the present study, the dramatic reduction in Ca^{2+} currents observed in the soma of *cac* neurons implies an important role of *cac* channels in other neuronal compartments as well. Previous neurite recording and Ca^{2+} imaging on cultured giant neurons have indicated a high Ca^{2+} current density along the neurites and in the terminals (Saito and Wu, 1991; Berke et al., 2006). In some cell bodies that do not support full-blown action potentials, spike activities in the distal compartments could still be detected as electrotonically degraded non-overshooting oscillations (Saito and Wu, 1991; Yao and Wu, 2001). However, in *cac* neurons, we did not detect any electrotonic spread of such spike activities from distal neurites, even under conditions that promote prolonged Ca^{2+} spikes (Fig. 3). Consistently, *in vivo* studies have demonstrated a role of *cac* channels in the function and development of axonal terminals of motor neurons. Mutations of *cac* result in greatly reduced synaptic transmission and restricted nerve terminal projection (Kawasaki et al., 2000, 2002, 2004; Rieckhof et al., 2003). Therefore, in the *Drosophila* nervous system, a single gene, *cac*, appears to play a major role to exert many short- and long-term Ca^{2+}-dependent regulations in neuronal development, function, and plasticity.

In vertebrates, different splice isoforms of Ca^{2+} channel α subunits display distinct physiological properties, drug sensitivities, phosphorylation, and subcellular distributions (Hell et al., 1994; Moreno Davila, 1999; Lipscombe et al., 2002). For instance, N-type channels, with high sequence similarity with *cac* (Rieckhof et al., 2003), have different isoforms with distinct voltage-dependent activation and decay kinetics (Stea et al., 1999). Therefore, the reported RNA splicing and editing of the *cac* transcripts (Smith et al., 1996, 1998) might account for the variation in voltage dependence and kinetics of Ca^{2+} currents mediated by *cac* channels. Additional investigations into additional *cac* alleles or heterologous expression of the identified splice variants may provide additional clues to the mechanisms underlying the remarkable functional diversity of Ca^{2+} currents generated by the *cac* gene.

References

Adelman JP, Shen KZ, Kavanaugh MP, Warren RA, Wu YN, Lagrutta A, Bond CT, North RA (1992) Calcium-activated potassium channels expressed from cloned complementary DNAs. Neuron 9:209–216.

Alkon DL (1999) Ionic conductance determinants of synaptic memory nets and their implications for Alzheimer's disease. J Neurosci Res 58:24–32.

Alkon DL, Shoukimas JJ, Heldman E (1982) Calcium-mediated decrease of a voltage-dependent potassium current. Biophys J 40:245–250.

Atkinson NS, Robertson GA, Ganetzky B (1991) A component of calcium-activated potassium channels encoded by the *Drosophila* slo locus. Science 253:551–555.

Baker K, Salkoff L (1990) The *Drosophila* Shaker gene codes for a distinctive K^+ current in a subset of neurons. Neuron 4:129–140.

Baro DJ, Levini RM, Kim MT, Willms AR, Lanning CC, Rodriguez HE, Harris-Warrick RM (1997) Quantitative single-cell-reverse transcription-PCR demonstrates that A-current magnitude varies as a linear function of shal gene expression in identified stomatogastric neurons. J Neurosci 17:6597–6610.

Berke B, Wu CF (2002) Regional calcium regulation within cultured *Drosophila* neurons: effects of altered cAMP metabolism by the learning mutations dunce and rutabaga. J Neurosci 22:4437–4447.

Berke BA, Lee J, Peng IF, Wu CF (2006) Sub-cellular Ca^{2+} dynamics affected by voltage- and Ca^{2+}-gated K^+ channels: regulation of the soma-growth cone disparity and the quiescent state in *Drosophila* neurons. Neuroscience 142:629–644.

Byerly L, Leung HT (1988) Ionic currents of *Drosophila* neurons in embryonic cultures. J Neurosci 8:4379–4393.

Byrne JH, Kandel ER (1996) Presynaptic facilitation revisited: state and time dependence. J Neurosci 16:425–435.

Cannon WB (1932) The wisdom of the body. New York: Norton.

Catterall WA (2000) Structure and regulation of voltage-gated Ca^{2+} channels. Annu Rev Cell Dev Biol 16:521–555.

Coetzee WA, Amarillo Y, Chiu J, Chow A, Lau D, McCormack T, Moreno H, Nadal MS, Ozaita A, Pountney D, Saganich M, Vega-Saenz de Miera E, Rudy B (1999) Molecular diversity of K^+ channels. Ann NY Acad Sci 868:233–285.

Cowan TM, Siegel RW (1984) Mutational and pharmacological alterations of neuronal membrane function disrupt conditioning in *Drosophila*. J Neurogenet 1:333–344.

Cowmeadow RB, Krishnan HR, Ghezzi A, Al'Hasan YM, Wang YZ, Atkinson NS (2006) Ethanol tolerance caused by slowpoke induction in *Drosophila*. Alcohol Clin Exp Res 30:745–753.

Davis GW, Bezprozvanny I (2001) Maintaining the stability of neural function: a homeostatic hypothesis. Annu Rev Physiol 63:847–869.

Drain P, Dubin AE, Aldrich RW (1994) Regulation of Shaker K^+ channel inactivation gating by the cAMP-dependent protein kinase. Neuron 12:1097–1109.

Eberl DF, Ren D, Feng G, Lorenz LJ, Van Vactor D, Hall LM (1998) Genetic and developmental characterization of Dmca1D, a calcium channel alpha1 subunit gene in *Drosophila melanogaster*. Genetics 148:1159–1169.

Elkins T, Ganetzky B, Wu CF (1986) A *Drosophila* mutation that eliminates a calcium-dependent potassium current. Proc Natl Acad Sci USA 83:8415–8419.

Engel JE, Wu CF (1998) Genetic dissection of functional contributions of specific potassium channel subunits in habituation of an escape circuit in *Drosophila*. J Neurosci 18:2254–2267.

Enyeart JJ, Mlinar B, Enyeart JA (1996) Adrenocorticotropic hormone and cAMP inhibit noninactivating K^+ current in adrenocortical cells by an A-kinase-independent mechanism requiring ATP hydrolysis. J Gen Physiol 108:251–264.

Ertel EA, Campbell KP, Harpold MM, Hofmann F, Mori Y, Perez-Reyes E, Schwartz A, Snutch TP, Tanabe T, Birnbaumer L, Tsien RW, Catterall WA (2000) Nomenclature of voltage-gated calcium channels. Neuron 25:533–535.

Gasque G, Labarca P, Reynaud E, Darszon A (2005) Shal and shaker differential contribution to the K^+ currents in the *Drosophila* mushroom body neurons. J Neurosci 25:2348–2358.

Gielow ML, Gu GG, Singh S (1995) Resolution and pharmacological analysis of the voltage-dependent calcium channels of *Drosophila* larval muscles. J Neurosci 15:6085–6093.

Gola M, Crest M (1993) Colocalization of active KCa channels and Ca^{2+} channels within Ca^{2+} domains in helix neurons. Neuron 10:689–699.

Guan Z, Saraswati S, Adolfsen B, Littleton JT (2005) Genome-wide transcriptional changes associated with enhanced activity in the *Drosophila* nervous system. Neuron 48:91–107.

Hell JW, Westenbroek RE, Elliott EM, Catterall WA (1994) Differential phosphorylation, localization, and function of distinct alpha 1 subunits of neuronal calcium channels. Two size forms for class B, C, and D alpha 1 subunits with different COOH-termini. Ann NY Acad Sci 747:282–293.

Hille B (2001) Ionic channels of excitable membranes. Sunderland, MA: Sinauer.

Jan YN, Jan LY, Dennis MJ (1977) Two mutations of synaptic transmission in *Drosophila*. Proc R Soc Lond B Biol Sci 198:87–108.

Jonas EA, Kaczmarek LK (1996) Regulation of potassium channels by protein kinases. Curr Opin Neurobiol 6:318–323.

Kawasaki F, Felling R, Ordway RW (2000) A temperature-sensitive paralytic mutant defines a primary synaptic calcium channel in *Drosophila*. J Neurosci 20:4885–4889.

Kawasaki F, Collins SC, Ordway RW (2002) Synaptic calcium-channel function in *Drosophila*: analysis and transformation rescue of temperature-sensitive paralytic and lethal mutations of cacophony. J Neurosci 22:5856–5864.

Kawasaki F, Zou B, Xu X, Ordway RW (2004) Active zone localization of presynaptic calcium channels encoded by the cacophony locus of *Drosophila*. J Neurosci 24:282–285.

Komatsu A, Singh S, Rathe P, Wu CF (1990) Mutational and gene dosage analysis of calcium-activated potassium channels in *Drosophila*: correlation of micro- and macroscopic currents. Neuron 4:313–321.

Kuromi H, Honda A, Kidokoro Y (2004) Ca^{2+} influx through distinct routes controls exocytosis and endocytosis at drosophila presynaptic terminals. Neuron 41:101–111.

Leung HT, Byerly L (1991) Characterization of single calcium channels in *Drosophila* embryonic nerve and muscle cells. J Neurosci 11:3047–3059.

Leung HT, Branton WD, Phillips HS, Jan L, Byerly L (1989) Spider toxins selectively block calcium currents in *Drosophila*. Neuron 3:767–772.

Linsdell P, Moody WJ (1994) Na^+ channel mis-expression accelerates K^+ channel development in embryonic *Xenopus laevis* skeletal muscle. J Physiol (Lond) 480:405–410.

Linsdell P, Moody WJ (1995) Electrical activity and calcium influx regulate ion channel development in embryonic *Xenopus* skeletal muscle. J Neurosci 15:4507–4514.

Lipscombe D, Pan JQ, Gray AC (2002) Functional diversity in neuronal voltage-gated calcium channels by alternative splicing of Ca_valpha1. Mol Neurobiol 26:21–44.

Llinas R, Steinberg IZ, Walton K (1981) Relationship between presynaptic calcium current and postsynaptic potential in squid giant synapse. Biophys J 33:323–351.

MacLean JN, Zhang Y, Johnson BR, Harris-Warrick RM (2003) Activity-independent homeostasis in rhythmically active neurons. Neuron 37:109–120.

Marder E, Prinz AA (2002) Modeling stability in neuron and network function: the role of activity in homeostasis. BioEssays 24:1145–1154.

Marrion NV, Tavalin SJ (1998) Selective activation of Ca^{2+}-activated K^+ channels by co-localized Ca^{2+} channels in hippocampal neurons. Nature 395:900–905.

McManus OB (1991) Calcium-activated potassium channels: regulation by calcium. J Bioenerg Biomembr 23:537–560.

Mee CJ, Pym EC, Moffat KG, Baines RA (2004) Regulation of neuronal excitability through pumilio-dependent control of a sodium channel gene. J Neurosci 24:8695–8703.

Moreno Davila H (1999) Molecular and functional diversity of voltage-gated calcium channels. Ann NY Acad Sci 868:102–117.

O'Dowd DK, Ribera AB, Spitzer NC (1988) Development of voltage-dependent calcium, sodium, and potassium currents in *Xenopus* spinal neurons. J Neurosci 8:792–805.

Peng IF, Wu CF (2007) Differential contributions of IA and IK subtypes to firing patterns in *Drosophila* culture neurons. J Neurophysiol, in press.

Poulain C, Ferrus A, Mallart A (1994) Modulation of type A K^+ current in *Drosophila* larval muscle by internal Ca^{2+}; effects of the overexpression of frequenin. Pflügers Arch 427:71–79.

Ren D, Xu H, Eberl DF, Chopra M, Hall LM (1998) A mutation affecting dihydropyridine-sensitive current levels and activation kinetics in *Drosophila* muscle and mammalian heart calcium channels. J Neurosci 18:2335–2341.

Rieckhof GE, Yoshihara M, Guan Z, Littleton JT (2003) Presynaptic N-type calcium channels regulate synaptic growth. J Biol Chem 278:41099–41108.

Robitaille R, Garcia ML, Kaczorowski GJ, Charlton MP (1993) Functional colocalization of calcium and calcium-gated potassium channels in control of transmitter release. Neuron 11:645–655.

Saito M, Wu CF (1991) Expression of ion channels and mutational effects in giant *Drosophila* neurons differentiated from cell division-arrested embryonic neuroblasts. J Neurosci 11:2135–2150.

Schmidt H, Luer K, Hevers W, Technau GM (2000) Ionic currents of *Drosophila* embryonic neurons derived from selectively cultured CNS midline precursors. J Neurobiol 44:392–413.

Schulz DJ, Goaillard JM, Marder E (2006) Variable channel expression in identified single and electrically coupled neurons in different animals. Nat Neurosci 9:356–362.

Singh A, Singh S (1999) Unmasking of a novel potassium current in *Drosophila* by a mutation and drugs. J Neurosci 19:6838–6843.

Singh S, Wu CF (1989) Complete separation of four potassium currents in *Drosophila*. Neuron 2:1325–1329.

Smith LA, Wang X, Peixoto AA, Neumann EK, Hall LM, Hall JC (1996) A *Drosophila* calcium channel alpha1 subunit gene maps to a genetic locus associated with behavioral and visual defects. J Neurosci 16:7868–7879.

Smith LA, Peixoto AA, Hall JC (1998) RNA editing in the *Drosophila* DMCA1A calcium-channel alpha 1 subunit transcript. J Neurogenet 12:227–240.

Spitzer NC (1999) New dimensions of neuronal plasticity. Nat Neurosci 2:489–491.

Stea A, Dubel SJ, Snutch TP (1999) alpha 1B N-type calcium channel isoforms with distinct biophysical properties. Ann NY Acad Sci 868:118–130.

Tanouye M, Ferrus A, Fujita S (1981) Abnormal action potentials associated with the Shaker complex locus of *Drosophila*. Proc Natl Acad Sci USA 78:6548–6552.

Turrigiano GG (1999) Homeostatic plasticity in neuronal networks: the more things change, the more they stay the same. Trends Neurosci 22:221–227.

Vergara C, Latorre R, Marrion NV, Adelman JP (1998) Calcium-activated potassium channels. Curr Opin Neurobiol 8:321–329.

von Schilcher F (1976) The behavior of cacophony, a courtship song mutant in *Drosophila melanogaster*. Behav Biol 17:187–196.

Wei A, Covarrubias M, Butler A, Baker K, Pak M, Salkoff L (1990) K^+ current diversity is produced by an extended gene family conserved in *Drosophila* and mouse. Science 248:599–603.

Wicher D, Walther C, Wicher C (2001) Non-synaptic ion channels in insects: basic properties of currents and their modulation in neurons and skeletal muscles. Prog Neurobiol 64:431–525.

Wright NJ, Zhong Y (1995) Characterization of K^+ currents and the cAMP-dependent modulation in cultured *Drosophila* mushroom body neurons identified by lacZ expression. J Neurosci 15:1025–1034.

Wu CF, Sakai K, Saito M, Hotta Y (1990) Giant *Drosophila* neurons differentiated from cytokinesis-arrested embryonic neuroblasts. J Neurobiol 21:499–507.

Yao WD, Wu CF (1999) Auxiliary Hyperkinetic beta subunit of K^+ channels: regulation of firing properties and K^+ currents in *Drosophila* neurons. J Neurophysiol 81:2472–2484.

Yao WD, Wu CF (2001) Distinct roles of CaMKII and PKA in regulation of firing patterns and K^+ currents in *Drosophila* neurons. J Neurophysiol 85:1384–1394.

Zhao ML, Wu CF (1997) Alterations in frequency coding and activity dependence of excitability in cultured neurons of *Drosophila* memory mutants. J Neurosci 17:2187–2199.

Zhao ML, Sable EO, Iverson LE, Wu CF (1995) Functional expression of Shaker K^+ channels in cultured *Drosophila*"giant" neurons derived from Sh cDNA transformants: distinct properties, distribution, and turnover. J Neurosci 15:1406–1418.

Zheng W, Feng G, Ren D, Eberl DF, Hannan F, Dubald M, Hall LM (1995) Cloning and characterization of a calcium channel alpha 1 subunit from *Drosophila melanogaster* with similarity to the rat brain type D isoform. J Neurosci 15:1132–1143.

Zhong Y, Wu CF (1993) Differential modulation of potassium currents by cAMP and its long-term and short-term effects: dunce and rutabaga mutants of *Drosophila*. J Neurogenet 9:15–27.